

# Fundamental limits on the rate of bacterial cell division

Nathan M. Belliveau<sup>†, 1</sup>, Griffin Chure<sup>†, 2, 3</sup>, Christina L. Hueschen<sup>4</sup>, Hernan G. Garcia<sup>5</sup>, Jane Kondev<sup>6</sup>, Daniel S. Fisher<sup>7</sup>, Julie A. Theriot<sup>1, 8</sup>, Rob Phillips<sup>2, 9, \*</sup>

\*For correspondence:

<sup>†</sup>These authors contributed equally to this work

<sup>1</sup>Department of Biology, University of Washington, Seattle, WA, USA; <sup>2</sup>Division of Biology and Biological Engineering, California Institute of Technology, Pasadena, CA, USA; <sup>3</sup>Department of Applied Physics, California Institute of Technology, Pasadena, CA, USA; <sup>4</sup>Department of Chemical Engineering, Stanford University, Stanford, CA, USA; <sup>5</sup>Department of Molecular Cell Biology and Department of Physics, University of California Berkeley, Berkeley, CA, USA; <sup>6</sup>Department of Physics, Brandeis University, Waltham, MA, USA; <sup>7</sup>Department of Applied Physics, Stanford University, Stanford, CA, USA; <sup>8</sup>Allen Institute for Cell Science, Seattle, WA, USA; <sup>9</sup>Department of Physics, California Institute of Technology, Pasadena, CA, USA; \*Contributed equally

**Abstract** This will be written next (promise).

## Relationship Between Cell Size and Growth Rate

The relationship between cell size and growth rate has long been of interest in the study of bacterial physiology, particularly following the now six decade-old observation that cell volume appears to increase exponentially with growth rate; known as Schaechter's growth law (*Schaechter et al., 1958; Taheri-Araghi et al., 2015*). However, the mechanism that governs this relationship, and even the question of whether the change in average cell size is truly exponential, has remained under debate (*Harris and Theriot, 2018*). Given the importance of cell size in determining the total protein mass that must be doubled (as well as in setting other parameters like the surface-area-to-volume ratio), we examine the influence size may have in setting the scales of protein abundance and growth dependence observed in the proteomic datasets.

As shown in ??(B), cells grow at a near-maximal rate dictated by their total ribosomal mass fraction  $\Phi_R$ , at least at moderate growth rates above  $0.5 \text{ hr}^{-1}$ , suggesting that growth rate could increased simply by making more ribosomes and increasing  $\Phi_R$ . In reality, however, large swaths of the proteome increase in absolute protein abundance as cells grow faster (Supplemental Figure X), and the ability to add additional ribosomes is likely constrained by other factors including crowding due to their large size (*Delarue et al., 2018; Soler-Bistué et al., 2020*). Rather, it is well-documented that *E. coli* cells add a constant volume per origin of replication (termed a "unit cell" or "initiation mass"), which is robust to a remarkable array of cellular perturbations (*Si et al., 2017*). To consider this in the context of the proteomic data, we used the measurements from *Si et al. (2017)* for wild-type *E. coli* cells grown in different nutrient conditions (*Figure 1(A)*) to estimate the average number of origins per cell  $\langle \# \text{ ori} \rangle$  across the data. Indeed, we find an approximately linear correlation between ribosome copy number and  $\langle \# \text{ ori} \rangle$  (*Figure 1(B)*).

The average number of origins  $\langle \# \text{ ori} \rangle$  is set by how often replication must be initiated per cell doubling under steady-state growth. This can be quantified as

$$\langle \# \text{ ori} \rangle = 2^{\tau_{\text{cyc}}/\tau} = 2^{\tau_{\text{cyc}}\lambda/\ln(2)}, \quad (1)$$

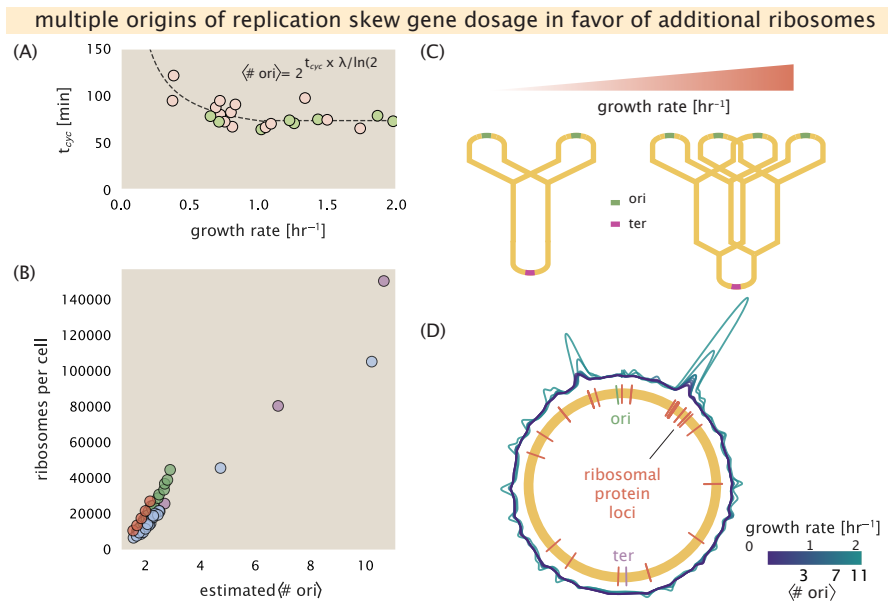


**Figure 1. Multiple replication initiations bias protein synthesis in favor of more ribosome.** (A) Experimental data from Si *et al.* (2017). Dashed line shows fit to the data, which were used to estimate  $\langle \# \text{ ori} \rangle$ .  $t_{\text{cyc}}$  was assumed to vary in proportion to  $\tau$  for doubling times great than 40 minutes, and then reach a minimum value of [fill in] minutes below this (see Supplemental Appendix X for additional details). Red data points correspond to measurements in strain MG1655, while light green points are for strain NCM3722. (B) Plot of the ribosome copy number estimated from the proteomic data against the estimated  $\langle \# \text{ ori} \rangle$ . (C) Schematic shows the expected increase in replication forks (or number of ori regions) as *E. coli* cells grow faster. (D) A running Gaussian average (20 kbp st. dev.) of protein copy number is calculated for each growth condition considered by (Schmidt *et al.*, 2016). Since total protein abundance increases with growth rate, protein copy numbers are median-subtracted to allow comparison between growth conditions.  $\langle \# \text{ ori} \rangle$  are estimated using the data in (A) and Equation 1. [still looking into how best to use this type of analysis]

where  $t_{\text{cyc}}$  is the cell cycle time (referring to the time from replication initiation to cell division), and  $\tau$  is the cell doubling time. For a constant cell cycle time, observed at growth rates above about 0.5 hr<sup>-1</sup> (Helmstetter and Cooper, 1968), Equation 1 states that  $\langle \# \text{ ori} \rangle$  will increase exponentially with the growth rate.

Why does *E. coli* add a constant volume per  $\langle \# \text{ ori} \rangle$ ? To gain insight on this phenomenological discovery and how it pertains to growth, we must consider how the proteome size and composition changes with respect to growth rate. In Figure 1(D), we consider the position-dependent protein expression across the chromosome for each of the growth conditions from Schmidt *et al.* (2016). Here, we calculated a running Gaussian average of protein copy number (20 kbp st. dev. averaging window) based on each gene's transcriptional start site, which were then median-subtracted to account for the differences in total protein abundance with each growth condition. Importantly, we find that the major deviations in protein copy number are largely restricted to regions of ribosomal protein genes, with substantially higher deviations observed for cells with high  $\langle \# \text{ ori} \rangle$  (teal), as compared to those with low  $\langle \# \text{ ori} \rangle$  (purple). This is particularly apparent for genes closer to the origin, where the majority of ribosomal proteins are found. This suggests that in addition to the linear scaling between protein abundance and  $\langle \# \text{ ori} \rangle$ , the relative ribosomal abundance is tuned in proportion to  $\langle \# \text{ ori} \rangle$ . Since growth rate depends specifically on the ribosomal fraction  $\Phi_R$ , this result suggests that cells are changing their size as a way to tune  $\Phi_R$  to match the available nutrient conditions.

## Alarhone-Mediated Regulation Controls the Rate of Protein Synthesis

The relationship between cell size, actively translating ribosomes, and growth rate, suggest that cell size and ribosome content is tuned as a means to match the biosynthetic capacity to the available nutrient conditions. An illustration of this principle can be seen in the recent work of *Dai et al. (2016)* where disruption of the major glucose uptake system through the deletion of *ptsG* limits carbon uptake and growth by a factor of two as well as reduces the ribosomal mass fraction by a factor of two. and growth, which is reduced about two-fold. This matches our intuition given a decrease in growth rate governed by ?? for a change in ribosomal fraction of this magnitude. In this final section, we formulate and explore a minimal model of growth rate control. We use it to quantitatively show how changes in ribosomal content and total proteomic mass will allow cells to maximize their growth rate according to the available nutrient conditions, which we generalize as a supply of amino acids.

To react to changes in nutrient conditions, bacteria rely on secondary-messenger molecules like (p)ppGpp, which cause global changes in transcriptional and translational activity. In *E. coli*, amino acid starvation causes the accumulation of de-acylated tRNAs at the ribosome's A-site, leading to a strong increase in (p)ppGpp synthesis activity by RelA (*Hauryliuk et al., 2015*). The corresponding dramatic decrease in active ribosomal fraction  $f_a$  that is now apparent for growth rates below about  $0.5 \text{ hr}^{-1}$  ( $f_a \approx 0.5$  at a growth rate of about  $0.3 \text{ hr}^{-1}$ , *Dai et al. (2016)*) indicates that (p)ppGpp also coordinates growth in poor nutrient conditions. Furthermore, (p)ppGpp can inhibit the initiation of DNA replication by mediating a change in transcriptional activity and the supercoiling state of the origin of replication (*Kraemer et al., 2019*). These observations all raise the possibility that, via (p)ppGpp, cells mediate the growth-rate dependent changes in ( $\# \text{ ori}$ ), cell size and ribosomal abundance (*Zhu and Dai, 2019; Büke et al., 2020*). Indeed, recent work in a (p)ppGpp deficient strain of *E. coli* found that cells exhibited a high ratio of ( $\# \text{ ori}$ ) to ( $\# \text{ ter}$ ) and cell size that was more consistent with a fast growth state where (p)ppGpp levels are normally low (*Fernández-Coll et al., 2020*).

To better understand how cells are able to maximize their growth rate under different extents of nutrient limitation, we proceed by assuming that the rate of elongation  $r_t$  depends only on the availability of amino acids (and, therefore, also amino-acyl tRNAs). It is at the level of amino acid synthesis and availability that we will assume cells adjust their ribosomal abundance and cell size (*Figure 2(A)*). Other molecular players required for translation like elongation factors and GTP are considered in sufficient abundance, which appear to be valid assumptions given our analysis of the proteomic data and energy production thus far.

## Ribosomal Elongation Rate and Cellular Growth Rate are Linked by Amino Acid Scarcity

For simplicity, we proceed by considering all amino acids as a single species, with an effective cellular concentration  $[AA]_{\text{eff}}$ . The rate of elongation  $r_t$  will depend on how quickly ribosomes can match codons with their correct amino-acyl tRNA, along with the subsequent steps of peptide bond formation and translocation. We therefore consider that elongation will depend on two course-grained timescales, 1) the time required to find and bind each correct amino-acyl tRNA, and 2) the remaining steps in peptide elongation that will not depend on the amino acid availability. The time to translate each codon is given by the inverse of the elongation rate  $r_t$ , which can be written as,

$$\frac{1}{r_t} = \frac{1}{k_{on}\alpha[AA]_{\text{eff}}} + \frac{1}{r_t^{\text{max}}}. \quad (2)$$

where we have assumed that the rate of binding by amino-acyl tRNA  $k_{on}$  is proportional to  $[AA]_{\text{eff}}$  by a constant  $\alpha$ . The second term on the right-hand side reflects our assumption that other steps in peptide elongation are not rate-limiting, with a maximum elongation rate  $r_t^{\text{max}}$  of about 17 amino acids per second *Dai et al. (2016)*. This can be rearranged more succinctly in terms of an effective

106 binding constant  $K_D = r_t^{\max}/(k_{on} a)$ , with the elongation rate now given by,

$$r_t = \frac{r_t^{\max}}{1 + K_D/[AA]_{\text{eff}}}. \quad (3)$$

107 During steady-state growth, the amino acid concentration is constant ( $d[AA]_{\text{eff}}/dt=0$ ), meaning  
 108 that synthesis and consumption are matched. The effective amino acid concentration  $[AA]_{\text{eff}}$  will  
 109 relate to the rate of amino acid synthesis (or import, for rich media) and/or tRNA charging, denoted  
 110 as  $r_{AA}$ , and the rate of consumption,  $r_t \times R \times f_a$  by,

$$\int_0^\tau \frac{d[AA]_{\text{eff}}}{dt} dt = \int_0^\tau ([r_{AA}] - [r_t \times R \times f_a]) dt, \quad (4)$$

111 where the time from 0 to  $\tau$  is a single cell doubling, and the square brackets indicate of concen-  
 112 tration per time. Integrating yields,

$$[AA]_{\text{eff}} = ([r_{AA}] - [r_t \times R \times f_a])\tau. \quad (5)$$

113 Alternatively, we can speak in terms of ribosome copy number by stating that for given unit  
 114 volume  $V$ ,  $[r_{AA}] = r_{AA}/(V N_A)$  and  $[r_t \times R \times f_a] = (r_t \times R \times f_a)/(V N_A)$ , where  $N_A$  is Avogadro's number.  
 115 Since  $\tau = \ln(2)/\lambda$ , which itself is related to the parameters  $r_t \times R \times f_a$  and the total number of amino  
 116 acids to be polymerized  $N_{AA}$ , **Equation 5** this can be rewritten as

$$[AA]_{\text{eff}} = \frac{\ln(2)N_{AA}}{V N_A} \left( \frac{r_{AA}}{r_t \times R \times f_a} - 1 \right). \quad (6)$$

117 By plugging in **Equation 6** into **Equation 3**, which also depends on  $r_t$ , we can solve for  $r_t$  explicitly.  
 118 Its solution are the roots of a quadratic equation, with the positive given by,

$$r_t = \frac{\sqrt{c^2 + 4ckr_t^{\max} - 2cr_t^{\max} + (r_t^{\max})^2} - c - r_t^{\max}}{2(k-1)}. \quad (7)$$

119 Here,  $c = r_{AA}/(Rf_a)$  and  $k = N_A V K_D / N_{AA}$ . In the final two subsections we use this model to explore  
 120 how the cellular metabolic capacity ( $r_{AA}$ ) constrains the maximum growth rate, and then explain an  
 121 apparent role of for (p)ppGpp in mitigating translational activity at slow growth, where the number  
 122 of ribosomes is in excess.

### 123 Optimal Growth Rate, Ribosomal Content, and Cell Size Depend on Nutrient Availability 124 and Metabolic Capacity.

125 The way we will explore this model is to constrain the set of parameters based on the growth-  
 126 rate dependent proteomic changes in the available data under nutrient limitation; namely, we will  
 127 restrict the values of  $R$ ,  $N_{aa}$ , and  $V$  to those associated with the growth conditions in **Schmidt et al.**  
 128 **(2016)**. We will then consider how changes in the nutrient conditions, through the parameter  $r_{aa}$ ,  
 129 influence the maximum growth rate. In **Figure 2(B)** we plot the elongation rate  $r_t$  for a high and  
 130 low value of  $r_{aa}$ , reflective of poor and rich nutrient conditions, respectively as a function of cellular  
 131 ribosome concentration [NB: need to state values used - maybe rationalize choice of values based  
 132 on the data]. Here we find that for high values of  $r_{aa}$ , cells will be able to support protein synthesis  
 133 and maintain a high rate of elongation. However, for poor nutrient conditions (low  $r_{aa}$ ), a high  
 134 abundance of ribosomes causes a dramatic decrease in  $r_t$ . In this regime, we see that a reduction  
 135 of actively translating ribosomes, through a decrease in the parameter  $f_a$ , allow cells to maintain  
 136 a high rate of elongation even under more pronounced limits of nutrient limitation. By decreasing  
 137  $f_a$ , through direct inhibition of available ribosomes, cells are able to maintain their pool of amino  
 138 acids, which is observed experimentally (considered further in Supplemental Section XX).

139 In **Figure 2(C)** we show that for a particular cell state (i.e. specific value of  $R$ ,  $N_{aa}$ , and  $V$ ), there  
 140 will be a maximal growth rate that depends on the capacity of the cell to provide amino acids to  
 141 ribosomes. Specifically, we see that the maximum growth rate  $\lambda$  increases with increasing  $r_{aa}$ , and  
 142 corresponds to a cell with higher ribosomal fraction. Importantly, however, there is an optimum

**Figure 2.** (A) (B)

---

143 set of  $R$ ,  $N_{aa}$ , and  $V$  that are strictly dependent on the value of  $r_{aa}$ . Increasing the ribosomal concen-  
144 tration beyond the cell's metabolic capacity has the adverse consequence of depleting the supply  
145 of amino acids and a concomitant decrease in the elongation rate  $r_i$  (**Figure 2(B)**).

## References

- Büke, F., Grilli, J., Lagomarsino, M. C., Bokinsky, G., and Tans, S. (2020). ppGpp is a bacterial cell size regulator. *bioRxiv*, 266:2020.06.16.154187.
- Dai, X., Zhu, M., Warren, M., Balakrishnan, R., Patsalo, V., Okano, H., Williamson, J. R., Fredrick, K., Wang, Y.-P., and Hwa, T. (2016). Reduction of translating ribosomes enables *Escherichia coli* to maintain elongation rates during slow growth. *Nature Microbiology*, 2(2):16231.
- Delarue, M., Brittingham, G. P., Pfeffer, S., Surovtsev, I. V., Pinglay, S., Kennedy, K. J., Schaffer, M., Gutierrez, J. I., Sang, D., Poterewicz, G., Chung, J. K., Plitzko, J. M., Groves, J. T., Jacobs-Wagner, C., Engel, B. D., and Holt, L. J. (2018). mTORC1 Controls Phase Separation and the Biophysical Properties of the Cytoplasm by Tuning Crowding. *Cell*, 174(2):338–349.e20.
- Fernández-Coll, L., Maciag-Dorszynska, M., Tailor, K., Vadia, S., Levin, P. A., Szalewska-Palasz, A., Cashel, M., and Dunny, G. M. (2020). The Absence of (p)ppGpp Renders Initiation of *Escherichia coli* Chromosomal DNA Synthesis Independent of Growth Rates. *mBio*, 11(2):45.
- Harris, L. K. and Theriot, J. A. (2018). Surface Area to Volume Ratio: A Natural Variable for Bacterial Morphogenesis. *Trends in microbiology*, 26(10):815–832.
- Hauryluk, V., Atkinson, G. C., Murakami, K. S., Tenson, T., and Gerdes, K. (2015). Recent functional insights into the role of (p)ppGpp in bacterial physiology. *Nature Reviews Microbiology*, 13(5):298–309.
- Helmstetter, C. E. and Cooper, S. (1968). DNA synthesis during the division cycle of rapidly growing *Escherichia coli* Br. *Journal of Molecular Biology*, 31(3):507–518.
- Kraemer, J. A., Sanderlin, A. G., and Laub, M. T. (2019). The Stringent Response Inhibits DNA Replication Initiation in *E. coli* by Modulating Supercoiling of *oriC*. *mBio*, 10(4):822.
- Schaechter, M., Maaløe, O., and Kjeldgaard, N. O. (1958). Dependency on Medium and Temperature of Cell Size and Chemical Composition during Balanced Growth of *Salmonella typhimurium*. *Microbiology*, 19(3):592–606.
- Schmidt, A., Kochanowski, K., Vedelaar, S., Ahrné, E., Volkmer, B., Callipo, L., Knoops, K., Bauer, M., Aebersold, R., and Heinemann, M. (2016). The quantitative and condition-dependent *Escherichia coli* proteome. *Nature Biotechnology*, 34(1):104–110.
- Si, F., Li, D., Cox, S. E., Sauls, J. T., Azizi, O., Sou, C., Schwartz, A. B., Erickstad, M. J., Jun, Y., Li, X., and Jun, S. (2017). Invariance of Initiation Mass and Predictability of Cell Size in *Escherichia coli*. *Current Biology*, 27(9):1278–1287.
- Soler-Bistué, A., Aguilar-Pierlé, S., Garcia-Garcera, M., Val, M.-E., Sismeiro, O., Varet, H., Sieira, R., Krin, E., Skovgaard, O., Comerci, D. J., Eduardo P. C. Rocha, and Mazel, D. (2020). Macromolecular crowding links ribosomal protein gene dosage to growth rate in *Vibrio cholerae*. *BMC Biology*, 18(1):1–18.
- Taheri-Araghi, S., Bradde, S., Sauls, J. T., Hill, N. S., Levin, P. A., Paulsson, J., Vergassola, M., and Jun, S. (2015). Cell-size control and homeostasis in bacteria. - PubMed - NCBI. *Current Biology*, 25(3):385–391.
- Zhu, M. and Dai, X. (2019). Growth suppression by altered (p)ppGpp levels results from non-optimal resource allocation in *Escherichia coli*. *Nucleic Acids Research*, 47(9):4684–4693.